Catal Lett (2016) 146:2215–2220
DOI 10.1007/s10562-016-1838-y

In Situ ATR-FTIR Investigation of Photodegradation of 3,4-Dihydroxybenzoic Acid on TiO_2

Xuefeng Hu[1] · **Thomas Bürgi**[2]

Received: 6 July 2016 / Accepted: 3 August 2016 / Published online: 11 August 2016

Abstract The catalytic photo-oxidation of 3,4-dihydroxybenzoic acid on TiO_2 has been studied by in situ ATR-FTIR in flowing water and in flowing wet air/nitrogen gas. In flowing water it was difficult to observe photodegradation intermediates despite photocatalytic action during UV illumination. In the flowing wet air/nitrogen system carboxylic acids and carbonates were observed. It was shown that water plays an important role in the formation of oxidation active species. Oxygen shows a prominent role for carboxylic acid degradation, but the photogenerated hole plays the important role for the 3,4-dihydroxybenzoic acid ring cleavage.

Graphical Abstract

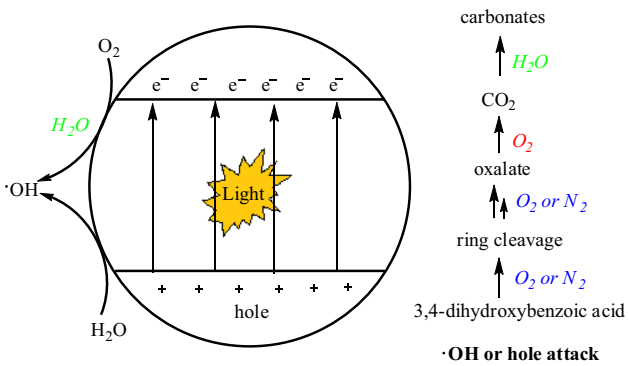

✉ Xuefeng Hu
xfhu@yic.ac.cn

[1] Key Laboratory of Coastal Environmental Processes and Ecological Remediation, Yantai Institute of Coastal Zone Research, Chinese Academy of Sciences, Yantai 264003, Shandong, People's Republic of China

[2] Département de Chimie Physique, Université de Genève, Quai Ernest-Ansermet 30, 1211 Genève 4, Switzerland

Keywords In situ spectroscopy · Photocatalysis · Attenuated total reflection · TiO_2 · 3,4-dihydroxybenzoic acid

1 Introduction

Photocatalysis on TiO_2 has attracted much attention especially in the field of environmental pollution abatement, such as air cleaning, self-cleaning windows and surfaces and waste water purification [1–3]. Air cleaning and self-cleaning typically rely on the adsorption of organic pollutants on TiO_2 which is illuminated by UV or solar light under certain humidity. In waste water purification the polluted water is flowed through a TiO_2 layer immobilized on a photoreactor under UV or solar light illumination. The catalytic activity is based on the photogeneration of electron—hole pairs in the semiconductor. These charge carriers either recombine inside the particle or move to its surface where they can react with adsorbed molecules. Holes usually oxidize organic compounds, inducing their oxidative degradation, while electrons mainly reduce molecular oxygen to superoxide radicals and then other reactive oxygen species, also leading to the degradation of organic compounds.

Among the large variety of environmental pollutants, aromatic compounds occupy an important place due to its toxicities and unusual stability. Catechol and its derivatives are important intermediates in the photo-degradation of benzene and its derivatives because OH radicals attack the aromatic ring before the latter is cleaved [4, 5]. The two hydroxyl groups of catechol and its derivatives lead to strong adsorption on TiO_2, which may be a crucial factor for the cleavage of the aromatic ring [6]. Aliphatic carboxylic acids are subsequently formed after the opening of aromatic ring, which also bind to TiO_2 [7]. The acids are then further

decomposed. For example it has been shown that succinate decomposes to malonate which leads to oxalate and finally CO_2 [8].

Attenuated total reflection infrared spectroscopy (ATR-FTIR) provides a sensitive tool for the analysis of surface-bound molecules, making it a powerful technique for the study of photocatalytic reactions taking place at the surface of a semi-conductor. In particular, the technique, which uses the evanescent field formed at the interface between an internal reflection element and the sample, enables one to study the corresponding interface in situ, i.e. during illumination and in the presence of liquid water.

In this paper 3,4-dihydroxybenzoic acid is used as a model organic compound and its photodegradation is studied by in situ ATR-FTIR in order to characterize the nature of the interface and its adsorbates during illumination. We furthermore focused on two main questions: (1) What are the roles of water and oxygen? (2) What kind of oxidizing agent plays the important role in opening of the aromatic ring and the mineralization of the aliphatic acid?

2 Experimental

2.1 Catalyst and Chemicals

Degussa P25 TiO_2, containing 80 % anatase and 20 % rutile with a surface area of 51 m^2/g and average primary particle size of 21 nm, was used in the photocatalysis experiments. 3,4-dihydroxybenzoic acid (Sigma–Aldrich, >97 %) was used as received. Nitrogen (N_2, 99.995 %) from CarbaGas, was used to remove oxygen from the reaction system.

2.2 Thin-Film Preparation

A slurry of the catalyst powder was prepared from 10 mg catalyst and 10 mL of water (Milli-Q, 18 MΩ cm). After sonication (Branson 200 ultrasonic cleaner) for 30 min, the mixture was spin coated onto a cleaned Ge internal reflection element (IRE) (52 × 20 × 2 mm; KOMLAS) at 1000 rpm for 2 min ten times. The as-deposited film was dried at 120 °C for 12 h. Scanning electron microscopy shows that this procedure leads to homogeneous films with an estimated film thickness on the order of one micrometer. Fresh films were prepared every day, and results were reproduced on different catalyst films. For experiments in flowing wet air the 3,4-dihydroxybenzoic acid was adsorbed on the TiO_2 film by immersing the film into 3,4-dihydroxybenzoic acid solution (4×10^{-5} M) for 1 h. The film was then washed with water to get rid of the weakly adsorbed 3,4-dihydroxybenzoic acid and blowed dry with nitrogen gas. Test experiments showed that no adsorption and no reaction took place (within the detection limit of the ATR-FTIR) in the absence of TiO_2.

2.3 In Situ Spectroscopy

ATR spectra were recorded with a dedicated flow-through cell, made from a Teflon piece, a fused silica plate (45 × 45 × 3 mm) with holes for the inlet and outlet (36 mm apart), and a flat (1 mm) viton seal. The cell was mounted on an attachment for ATR measurements within the sample compartment of a Bruker Equinox-55 FTIR spectrometer equipped with a narrow-band MCT detector. Spectra were recorded at 4 cm^{-1}. 200 scans were accumulated for one spectrum. For experiments in flowing liquid water, the reactant solution was passed through the cell and over the catalyst at a flow rate of 0.2 mL/min by means of a peristaltic pump (Ismatec, Reglo 100) located in front of the cell. For the experiments with flowing wet air/nitrogen water was heated at a certain temperature within a bottle with two inlets/outlets in order to saturate the vapor phase. The water vapor was then driven over the sample using a peristaltic pump at 0.2 ml/min. The water vapor was cooled to 20 °C before entering the cell.

For irradiation of the sample, UV light was provided by a 75 W Xenon arc lamp. The UV light from the source was guided to the ATR-IR cell via two fiber bundles. The light was passed through a 5-cm water filter to remove any infrared radiation. A Schott UG 11 (50 × 50 × 1 mm) broadband filter from ITOS was used to remove visible light (transmission at 270–380 nm). The irradiance at the sample was slightly below 10 mW/cm^2.

3 Results and Discussion

3.1 Adsorption and Desorption of 3,4-Dihydroxybenzoic Acid

ATR-FTIR is a valuable tool to characterise in detail the surface state of solid particles, and a detailed characterisation of the evolution of surface speciation will help the understanding of the involved mechanisms and therefore facilitate the improvement of the photomineralisation processes. In the ATR-FTIR spectrum of 3,4-dihydroxybenzoic acid the peak at 1288 cm^{-1}, assigned to the Ph-OH bending vibration, disappeared upon adsorption but a new strong peak appeared at 1278 cm^{-1} as shown in Fig. 1 (A) and (B) [9]. This strong peak corresponds to the Ph-O-Ti vibration, which indicates that 3,4-hydroxybenzoic acid is present on the TiO_2 surface as catecholate, in which the two oxygens in the phenolic groups coordinate with one Ti atom [10, 11]. The two bands in Fig. 1 (B) at 1517 cm^{-1} and 1370 cm^{-1} were assigned to the ν_{as} (COO^-) and the ν_s(COO^-) of the adsorbed molecule [9]. These two bands disappear when the solution pH was lowered to 1.5, while a new peak at 1703 cm^{-1} assign to ν(C = O) appears. In solution the corresponding peak is observed at 1688 cm^{-1}. Thus, the adsorbed

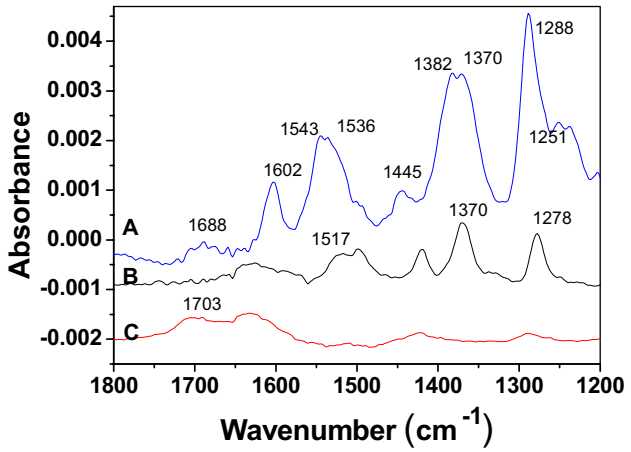

Fig. 1 ATR-FTIR spectra of 3,4-dihydroxybenzoic acid in solution (*A*) (10^{-2} M, pH 6.5) and adsorbed onto TiO_2 from 4×10^{-5} M aqueous solution at pH 6.5 (*B*) and pH 1.5 (*C*)

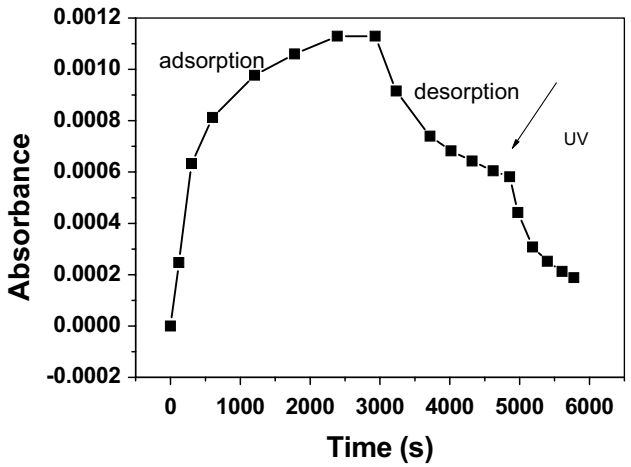

Fig. 2 Time profile of the absorbance at 1278 cm^{-1} during adsorption, desorption and UV light illumination. During the adsorption process a solution of 4×10^{-5} M 3,4-hydroxybenzoic acid at pH 6.5 was flowed through the cell and over the TiO_2 film. During desorption and UV light illumination processes water at pH 6.5 was flowed

3,4-dihydroxybenzoic acid may undergo deprotonation/protonation at the –COOH moiety, suggesting that this group is not involved in complexation of Ti atoms [10].

The 3,4-hydroxybenzoic acid attained dark adsorption equilibrium after about 40 min as seen from Fig. 2, where the absorbance at 1278 cm^{-1} is plotted as a function of time. When subsequently flowing water over the sample one part of the adsorbed molecules leave the surface. Within 30 min about 50 % is desorbing, but after that desorption of 3,4-dihydroxybenzoic acid from TiO_2 is slow when rinsing with water at pH 6.5. This indicates the presence of two differently adsorbed species, one desorbing faster than the other. One possible interpretation of this finding is the presence of a chemisorbed species with the formation Ph-O-Ti, which is difficult to desorb by flowing water over the sample. The other species may be physisorbed interacting with the surface through ionic bonds, hydrogen bonds, electrostatic interaction or van der Waals force [12]. Upon UV irradiation also the chemisorbed species is removed from the surface as can be seen in Fig. 2.

An indication on the strength of adsorbate binding can be obtained from isotherm data. Assuming a Langmuir isotherm and that the measured absorbance is directly proportional to the amount adsorbed, which is a good approximation, the following equation can be derived [13]:

$$C_0/A = C_0/A_{max} + 1/(A_{max}K) \quad (1)$$

Here C_0 is the concentration of 3,4-dihydroxybenzoic acid in solution, A is the measured absorbance of the adsorbed 3,4-dihydroxybenzoic acid, A_{max} is the absorbance for maximum coverage and K is the equilibrium constant for adsorption. Figure 3 shows the adsorption isotherms of 3,4-dihydroxybenzoic acid from 10^{-5} to 2×10^{-4} M on TiO_2 at pH 6.5. C_0/A vs. C_0 plots constructed from the absorbance band at 1278 cm^{-1} in the spectra gave a straight line as shown in Fig. 4. From this the maximum coverage absorbance $A_{max} = 0.0013$ and Langmuir adsorption constant $K = 1.5\times10^5\ M^{-1}$ were obtained thus demonstrating that the adsorption is quite strong.

3.2 Photodegradation in Flowing Water

Figure 5 shows ATR-FTIR spectra recorded during the photodegradation of 3,4-dihydroxybenzoic acid. The spectra were recorded after adsorption of the molecule till full coverage and after desorption in flowing water. This leaves behind on the surface only the strongly adsorbed species. The spectrum recorded just before starting UV illumination was taken as the background. Negative signals of 3,4-dihydroxybenzoic acid becoming more prominent with illumination time indicate the removal 3,4-dihydroxybenzoic acid from TiO_2. Upon illumination and photodegradation of 3,4-dihydroxybenzoic acid a new band at 1638 cm^{-1} is observed in the ATR-FTIR spectra, which is assigned to the bending mode from water that replaces 3,4-dihydroxybenzoic acid on the TiO_2 surface [14]. No significant bands that could be associated with intermediates of the photodegradation of 3,4-dihydroxybenzoic acid were observed.

Phenol derivatives usually mineralize to CO_2 over TiO_2 with carboxylic acid and dicarboxylic acid as intermediates [15]. There is no clear evidence of carboxylic acid absorption in the spectra, which might be partly due to spectral overlap between the bands of 3,4-dihydroxybenzoic acid on TiO_2 and the ν_{as}(COO) and ν_s(COO) bands of the acids. Also, under the flowing water conditions applied here the acids are removed fast from the evanescent field.

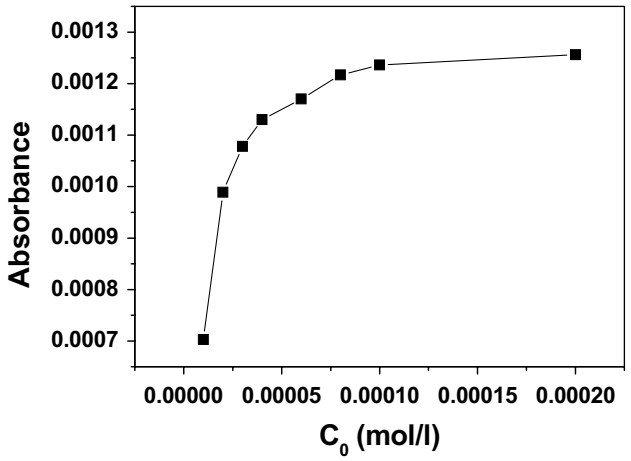

Fig. 3 Absorbance at 1278 cm^{-1} of 3,4-dihydroxybenzoic acid adsorbed onto TiO_2 in the dark at pH 6.5 as a function of concentration in solution. The values were measured while flowing a solution of 3,4-dihydroxybenzoic acid at the respective concentration over the sample for 40 min

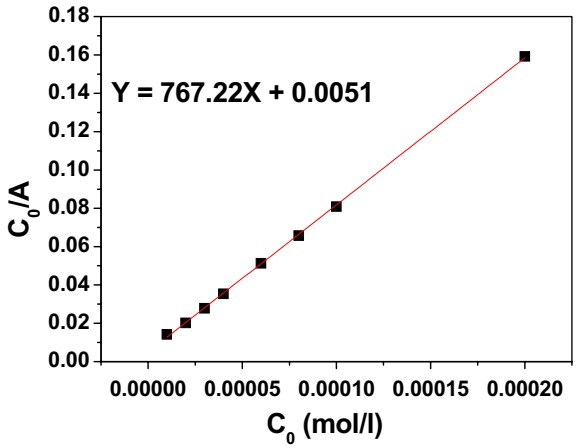

Fig. 4 Plot of C_0/A versus C_0, where C_0 is the concentration in solution and A is the absorbance of the ATR-FTIR spectra at 1278 cm^{-1} associated with adsorbed 3,4-dihydroxybenzoic acid. The straight line corresponds to the Langmuir isotherm model

Furthermore, the degradation of carboxylic acids should be fast under the applied conditions, which leads to a low concentration of acids on the surface [16]. However, as shown in Fig. 6 the bands at 1278 and 1372 cm^{-1} decrease at different rates under UV illumination, the 1278 cm^{-1} band decreasing faster. This is at least an indication that at 1372 cm^{-1} a spectral overlap occurs with a species that is formed during illumination such as the ν_s(COO) band of carboxylic acids. One prominent species on the TiO_2 surface during photocatalytic degradation of carboxylic acids is oxalate. This species is almost at the end of the degradation chain and shows prominent signals around 1700 cm^{-1}. In the spectra in Fig. 5 only a small signal is observed in this spectral region.

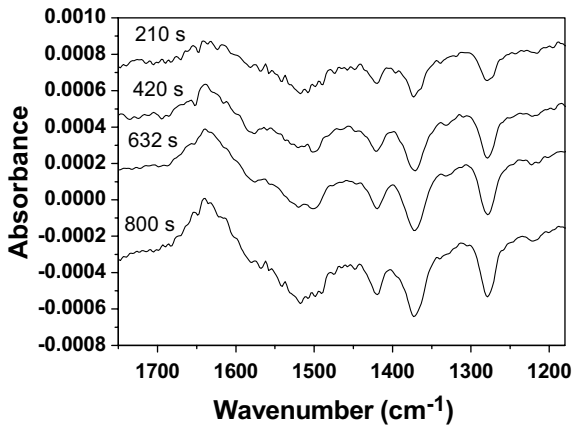

Fig. 5 ATR-FTIR spectra as a function of time recorded during UV light illumination of adsorbed 3,4-dihydroxybenzoic acid on TiO_2 while flowing water at pH 6.5. As the background for the absorbance spectra served the spectrum recorded just before illumination

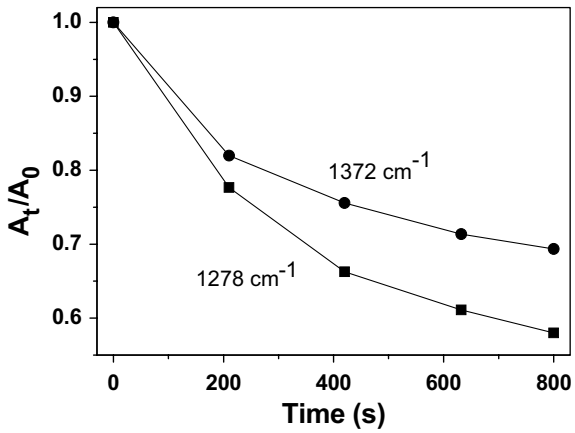

Fig. 6 Time profile of the absorbance bands at 1278 and 1372 cm^{-1} under UV illumination. The signals were scaled to 1.0 at the beginning of illumination by dividing the absorbance A_t at time t by the absorbance A_0 at the beginning of the experiment

3.3 Effects of Water on Photodegradation

In an attempt to understand the influence of liquid water on the photooxidation of 3,4-dihydroxybenzoic acid and to capture possible photodegradation intermediates, the UV illumination of adsorbed 3,4-dihydroxybenzoic acid on TiO_2 was performed in wet air containing different amounts of water.

Under wet air conditions the Ph-O-Ti vibration observed at 1278 cm^{-1} in aqueous solution shifts to 1266 cm^{-1} as shown in Fig. 7. The shift may be caused by a loss of hydrogen bonding interactions and/or redistribution of electron density within the organic molecule [17]. The absorbance band at 1638 cm^{-1} associated with adsorbed water increased with time of photodegradation of 3,4-dihydroxybenzoic acid and increase of water content in air flow through the cell, which is controlled by the temperature in the water saturation system. The rate of photodegradation of 3,4-dihydroxybenzoic

acid, as measured by the decrease of the absorbance band at 1266 cm^{-1}, increased with the water content on the TiO_2 surface.

Organic pollutants can be oxidized in different ways over TiO_2 photocatalyst. The absorption of a photon with energy larger than the band gap of TiO_2 can excite an electron from the valence band to the conduction band thus producing reductive conduction band electrons and oxidative valence band holes [18]. The holes can react with adsorbed water to produce OH radicals or directly oxidize adsorbed organic pollutants to their radicals. In the presence of oxygen, the conduction band electrons are usually scavenged by O_2 to yield superoxide radical anions and H_2O_2, which are involved in the production of OH radicals in aqueous solution [19]. The formation of OH radicals and other reactive oxygen species via the two pathways described above requires water. The rate of the photocatalytic oxidation pathway of 3,4-dihydroxybenzoic acid via OH radicals is thus expected to depend on the water content on the TiO_2 surface. A faster rate is expected in higher humidity air. Figure 7 supports this idea. At higher levels of adsorbed water, as evidenced by the band at 1638 cm^{-1}, the photodegradation of 3,4-dihydroxybenzoic acid is faster, as shown by the band at 1266 cm^{-1}.

The signal in Fig. 7 at 1720 cm^{-1} as a shoulder in the high water content spectrum or at 1708 cm^{-1} at low water content is assigned to oxalate on TiO_2 in different adsorption modes and different surface environment [20, 21]. This indicates that oxalate is one of the most important intermediates of 3,4-dihydroxybenzoic acid photodegradation and it could be one of the bottlenecks in the complete mineralization of 3,4-dihydroxybenzoic acid to CO_2. At high water content, see top spectrum in Fig. 7, there is some evidence for carbonates on the surface. There are two broad bands slightly below 1600 cm^{-1} and slightly above 1300 cm^{-1} and a sharper band at 1317 cm^{-1} that might be assigned to carbonates [8, 22]. Carbonates can be formed from CO_2, which is the final photodegradation product. The spectra in Fig. 7 indicate that carbonates can only be formed at higher water levels. This could mean that the carbonates form already in the water phase and adsorb on TiO_2 as such, in contrast to being formed directly on the TiO_2 surface.

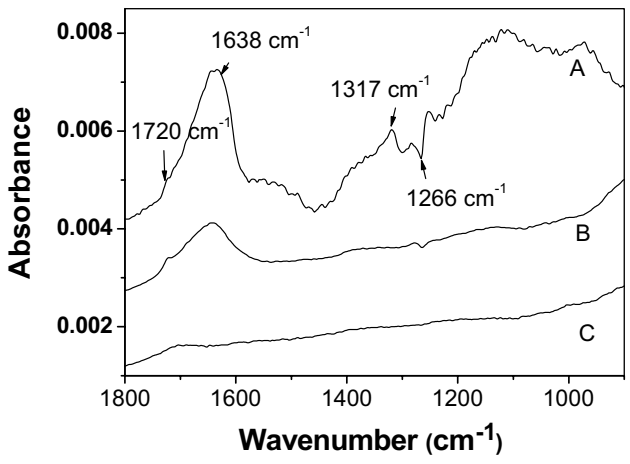

Fig. 7 ATR-FTIR spectra of 3,4-dihydroxybenzoic acid photodegradation after 45 min UV illumination with air purged water vapor at different water saturation temperatures: *A*, 50 °C; *B*, 35 °C; *C*, 20 °C. Note that the sample was at room temperature for all experiments. The spectrum recorded before UV illumination was taken as the background

3.4 Effects of Oxygen on Photodegradation

As mentioned above oxygen plays an important role as electron acceptor and in the formation of reactive oxygen species, which usually promote the photodegradation of organic pollutants. It was reported that molecular oxygen is the ultimate ring-opening agent of 3,5-di-tert-butylcatechol in TiO_2 photocatalysis using water/acetonitrile mixed solvent [6]. However, the photodegradation of 3,4-dihydroxybenzoic acid observed in the absence of oxygen as can be seen from Fig. 8 by monitoring the absorbance at 1266 cm^{-1}. There is a broad band appearing at 1630 ~ 1540 cm^{-1} and several peaks at 1463 ~ 1327 cm^{-1}, which can be assigned to the ν_{as}(COO) and ν_s(COO) vibrations, respectively, of various carboxylic acids [23, 24]. The absorbance at 1708 cm^{-1} is assigned to oxalate. The broad peak above 1700 cm^{-1} is due to the C = O stretching vibration of various carboxylic acids [23, 24]. Taking into account the findings described in ref. 6, different ring-opening mechanisms may occur depending on the structure of organic compound and the solvent. On the one hand, electronic effect of substituents on the aryl ring plays an important role in the catechol dioxygenation and subsequent ring-opening reaction, and the electron-donating substituents would facilitate this reaction [25]. On the other hand, the existence of organic solvent may affect the formation of OH radicals.

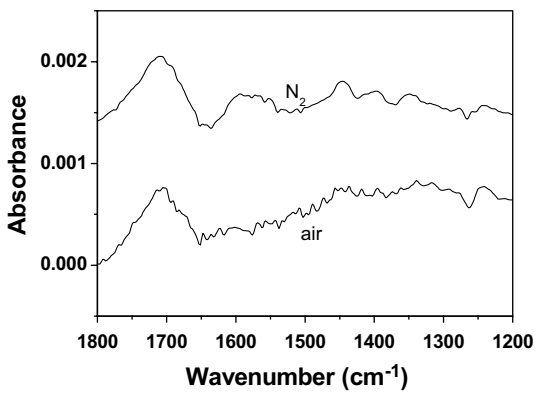

Fig. 8 ATR-FTIR of 3,4-dihydroxybenzoic acid photodegradation after 200 min UV illumination with air and N_2 purged water vapor at 20 °C. The sample before UV illumination served as the background

The above observations indicate that photodegradation of 3,4-dihydroxybenzoic acid proceeds via three main steps: first, the aromatic ring is cleaved and various aliphatic carboxylic acids are formed; second, the aliphatic acids shorten its hydrocarbon chain to form oxalate [8] and finally the oxalate is also transformed to CO_2. The rates of the various reaction steps can be influenced by oxygen mainly in two ways. Oxygen acts as an acceptor for the electron of the photogenerated electron–hole pair. The resulting reactive oxygen species can directly attack adsorbed molecules. Furthermore, the acceptance of the electron leads to an increased life time of the photogenerated hole. The photodegradation rate of 3,4-dihydroxybenzoic acid and its photodegradation intermediate products would decrease in the absence of oxygen. The hole will be the only oxidation center in the absence of oxygen, reacting with surface adsorbed water to produce OH radicals or directly oxidize adsorbed organic.

The spectra in Fig. 8 show that the 3,4-dihydroxybenzoic acid ring opening reaction is observed in the presence and absence of oxygen, but much more carboxylic acid are formed in the absence of oxygen. This suggests that hole oxidation plays a prominent role in the ring open reaction of 3,4-dihydroxybenzoic acid, but oxygen and reactive oxygen species play a more important roles in the consecutive shortening of the hydrocarbon chain.

4 Conclusion

3,4-dihydroxybenzoic acid shows strong absorption on TiO_2, which provides the possibility for photodegradation under TiO_2 catalysis. Water and oxygen play important roles for the reaction rate as well as the relative rate of different reaction pathways, which is determined by the formation of reactive oxidation species. The photodegradation rate of 3,4-dihydroxybenzoic acid increased with increasing the content of water vapor in air. Absence of oxygen decreased the photodegradation of 3,4-dihydroxybenzoic acid but increased the intermediate products formed on TiO_2. ATR-FTIR provides detailed information about the time evolution of the photocatalytic surface during illumination.

Acknowledgments The generous financial support by the National Science Foundation of China (nos. 41076040 and 41230858) is gratefully acknowledged.

References

1. Nath RK, Zain MFM, Jamil M (2016) Renew Sust Energ Rev 62:1184
2. Zhang W, Jia BP, Wang QZ, Dionysiou DD (2015) J Nanopart Res 17:221
3. Powell MJ, Quesada-Cabrera R, Taylor A, Teixeira D, Papakonstantinou I, Palgrave RG, Sankar G, Parkin IP (2016) Chem Mater 28:1369
4. Bhatkhande DS, Pangarkar VG, Beenackers AACM (2001) J Chem Technol Biotechnol 77:102
5. Ji HH, Chang F, Hu XF, Qin W, Shen JW (2013) Chem Eng J 218:183
6. Pang XB, Chang W, Chen CC, Ji HW, Ma WH, Zhao JC (2014) J Am Chem Soc 136:8714
7. Hu XF, Buergi T (2012) Appl Catal A 449:139
8. Dolamic I, Buergi T (2007) J Catal 248:268
9. Borah JM, Sarma J, Mahiuddin S, Colloid Surf A 387:50
10. Araujo PZ, Morando PJ, Blesa MA (2005) Langmuir 21:3470
11. Guan XH, Shang C, Chen GH (2006) Chemosphere 65:2074
12. Qin L, Shi WP, Liu WF, Yang YZ, Liu XG, Xu BS (2016) RSC Adv 6:12504
13. Dobson KD, McQuillan AJ (1997) Langmuir 13:3392
14. Sheng H, Zhang HN, Song WJ, Ji HW, Ma WH, Chen CC, Zhao JC (2015) Angew Chem Int Ed 54:5905
15. Yang J, Dai J, Chen CC, Zhao JC (2009) J Photochem Photobiol A 208:66
16. Subramanian V, Pangarkar VG, Beenackers AACM (2000) Clean Prod Process 2:149
17. Hay MB, Myneni SCB (2007) Geochim Cosmochim Acta 71:3518
18. Guo YG, Lou XY, Xiao DX, Xu L, Wang ZH, Liu JS (2012) J Hazard Mater 241–242:301
19. Yuan R, Ramjaun NS, Wang Z, Liu J (2012) Chem Eng J 192:171
20. Hug SJ, Sulzberger B (1994) Langmuir 10:3587
21. Araujo PZ, Mendive CB, Garcia Rodenas LA, Morando PJ, Regazzoni AE, Blesa MA, Bahnemann D (2005) Colloid Surf A 265:73.
22. Mino L, Zecchina A, Martra G, Rossi AM, Spoto G (2016) Appl Catal B 196:135
23. Ojamae L, Aulin C, Pedersen H, Kall P (2006) J Colloid Interface Sci 296:71
24. Kubicki JD, Schroeter LM, Itoh MJ, Nguyen BN, Apitz SE (1999) Geochim Cosmochim Acta 63:2709
25. Lin G, Reid G, Bugg TDH (2001) J Am Chem Soc 123:5030